Challenges in Extending Optical Fibre Transmission Bandwidth Beyond C+L Band and How to Get There

Henrique Buglia, Eric Sillekens, Anastasiia Vasylchenkova, Wenting Yi,
Robert Killey, Polina Bayvel and Lidia Galdino
Optical Networks Group, Department of Electronic and Electrical Engineering
UCL (University College London)
London, United Kingdom
henrique.buglia.20@ucl.ac.uk

***Abstract*—Recently, we demonstrated a record single-mode fibre net throughput of 178.08 Tbit/s. In this paper, we model this experiment, investigating the main limitations and challenges behind this total throughput, together with the details of some approaches to overcome them, and an outlook for the future ultra-wideband network design and optimisation.**

***Index Terms*—Ultra-wideband system, ISRS GN-model, analytical modelling, WDM.**

I. Introduction

DATA rates in optical communications system have been dramatically increased. Strategies aim to increase total throughput are currently being developed. One of these strategies is to expand single-mode fibre (SMF) transmission bandwidth beyond C+L window. This strategy allows increasing fibre link and network capacities, in order to fully exploit existing SMF infrastructure.

A key technology required to expand transmission bandwidth is optical amplifiers, needed to compensate for fibre loss on a given transmission window. Different types of amplification schemes, such as Raman amplification, rare-earth doped fibre amplifiers and semiconductor optical amplifiers (SOA) have been used to expand optical fibre transmission window. Figure 1 illustrates the total throughput achieved by these technologies whether used alone or in combination [1]. Using Raman amplifiers and rare-earth doped fibre amplifiers, we demonstrated the world record transmission of 178.08 Tbit/s over 40 km [1]. This achievable throughput was obtained by simultaneously transmitting 16.83 THz bandwidth at the S-, C- and L-bands, together with adaptive modulation formats tailored with the received SNR and geometric shaping (GS), aiming to maximize the total throughput.

In this work, through experimental analysis and theoretical modelling, we investigate the main limitations that dictated this record throughput. We aim to investigate whether the experiment conceived in [1] was operated in optimum conditions. The impact of the back-to-back implementation penalty on the overall system performance is investigated as well as the signal power operation. The inter-channel stimulated Raman scattering Gaussian noise (ISRS GN) model was used to estimate the transmission system performance [12]. A particle swarm optimisation (PSO) [13] and a gradient descendent algorithm were implemented to find the optimum power per channel in the presence of ISRS, aimed to achieve the maximum total SNR and total throughput at the receiver. The system performance for optimum launch power per channel is then compared with the signal launched power used in the experiment [1].

This work is partly funded by the EPSRC project TRANSNET (EP/R035342/1). AV acknowledges the support of the Leverhulme Trust Early Career Fellowship (ECF-2020-150). H. Buglia is funded by EPSRC Microsoft grant EP/T517793/1. Dr L. Galdino is supported by the Royal Academy of Engineering.

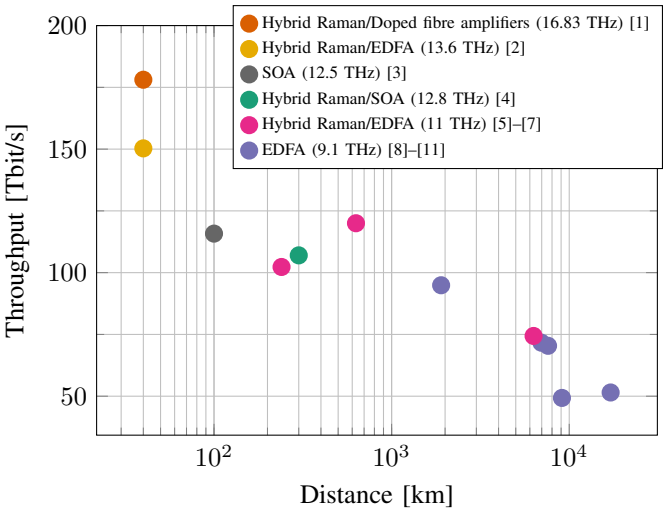

Fig. 1. Record data throughput versus distance for single mode fibre, not including spectral gaps between amplifier gain bandwidths [1].

II. Transmission System Under Investigation

In order to model the experiment in [1] and accurately predict its performance, the impairments arising from the transceiver (TRX), optical amplifiers to compensate for the fibre loss, and fibre nonlinearity must be taken into account. Assuming that all three impairment factors can be modelled as statistically independent additive noise sources, the total received SNR for the i-th channel (SNR_i) is expressed as

$$\mathrm{SNR}_i = \frac{P_i}{\kappa_i P_i + P_{\mathrm{ASE}_i} + \eta_n(f_i) P_i^3}, \tag{1}$$

978-3-903176-33-1

TABLE I
AMPLIFICATION SCHEME SUB-BANDS WITH CORRESPONDING NOISE PROPERTIES AND IMPLEMENTED MODULATION FORMATS

Sub-band [nm]	**$\mathrm{NF_{ASE}}$ [dB]**	**GS-QAM**	$\mathrm{SNR_{TRX}}$ **[dB]**
1484.86 - 1519.8	7.0	256-QAM	15.80
1520 - 1529	9.0	64-QAM	17.82
1529.2 - 1568	5.5	1024-QAM	21.25
1568.2 - 1607.8	6.0	1024-QAM	21.25
1608 - 1619.67	9.0	256-QAM	17.07

where i is the channel under consideration, P_i is the launch power, $\kappa_i = 1/\mathrm{SNR}_{\mathrm{TRX}_i}$ is the transceiver SNR, P_{ASE_i} is the amplified spontaneous emission (ASE) noise power calculated as [14, Eq. 10], and $P_{\mathrm{NLI}_i} = \eta_n(f_i)P_i^3$ is the non linear interference (NLI) noise power. The NLI coefficient $\eta_n(f_i)$ experienced by the channel of frequency f_i is calculated using the closed-form ISRS GN model proposed in [12]. This model is well suitable for modelling ultra-wideband transmission systems, and its accuracy compared to nonlinear Schrodinger equation (NLSE) simulations has been demonstrated at [12], [14].

The details of the transmission system under investigation are described in [1]. The system is based on WDM of N_{ch}=660 channels, each channel carries 25 GBd of information and is spaced by 0.5 GBd from its neighbour, in a total bandwidth of 16.83 THz (134.81 nm), ranging from 1484.86 nm to 1619.67 nm. The channels are transmitted over a single span of 40 km standard SMF with attenuation profile $\alpha(f_i)$ as [1, Fig. 2]. Total power of 20.4 dBm is launched into the fibre and the relative power per channel is also shown in [1, Fig. 2].

As per the experiment [1, Fig. 3,4], to maximize the total throughput, different GS quadrature amplitude modulations (GS-QAM) formats are used per amplification sub-band depending on the SNR obtained (see Table I). These modulation formats are taken into account on the ISRS GN model in order to calculate the values of the excess kurtosis (Φ_i) in the closed-form expressions of [12], used to estimate $\eta_n(f_i)$ for each channel. The modulations are the same as the ones designed in [1, Fig. 3].

The in-line amplifiers, used to compensate for fibre loss, were modelled with dynamic gain equalisation which fully compensates the power loss per channel. For each amplifier, the same noise figures ($\mathrm{NF_{ASE}}$) as the ones reported in [1, Sec. II] is used. These values are shown in Table I. It was assumed that each amplifier has the same NF across its entire gain bandwidth.

The back-to-back implementation penalty ($\mathrm{SNR_{TRX}}$) has not been measured experimentally for every channel separately. The $\mathrm{SNR_{TRX}}$ of few channels across the entire bandwidth were measured and the mean $\mathrm{SNR_{TRX}}$ per received amplifier sub-band, as shown in Table I, were used to estimate the system performance.

III. LAUNCH POWER OPTIMISATION

This section is devoted to finding the optimum launch power per channel for the transmission system under investigation. It should be noted that $\eta_n(f_i)$ is a function of the normalised launch power distribution and due to the presence of ISRS, the dynamic gain provided by each amplifier becomes dependent on the signal launch power (as it needs to account the Raman transfer power of low wavelengths to high wavelengths), therefore, P_{ASE} also becomes frequency-dependent. For these reasons, the signal launch power optimisation needs to be carried out simultaneously for all the channels. This creates to a N_{ch}-dimensional optimisation problem. Additionally, in the presence of ISRS, this optimisation is non-convex, leading to multiple local solutions [14].

We use the model described in Section II to compute a local optimal solution of the non-convex optimisation problem described above. To that end, we use the particle swarm optimisation (PSO) [13] combined with a gradient descent algorithm with a back straight line search. The parameters of these algorithms were the same as those described in [14, Sec. IV].

The PSO is efficient in exploring the N_{ch}-dimensional optimisation space, but inaccuracy in finding exact minima. To provide this accuracy, the solution of the PSO is used as initial solution for the gradient descent algorithm, which is known to converge to a local minimum if a good initial solution is provided. Therefore, the combination of these both algorithms provides a good balance between global and local search [14, Sec. IV]. In order to reduce the complexity, groups of 5 adjacent channels are lumped into one super-channel. Finally, as the optimum launch power is independent of the transceiver noise, the cost function used is the sum of the Additive White Gaussian Noise (AWGN) capacities over all the channels considering an ideal transceiver.

Figure 2 shows the optimum launch power for each channel (green line), resulting in a total launch power of 21.93 dBm, as well as the signal power profile used on the experiment [1] (red line), with a total launch power of 20.4 dBm. The optimum spectrally uniform power (blue line), with a total launch power of 20.95 dBm was also computed for comparison. Different background colours are used to illustrates the different values of $\mathrm{NF_{ASE}}$ for the in-line amplifiers used across different sub-band within the transmission bandwidth as shown in Table I.

For the optimum launch power per channel profile optimisation (green line), a maximum power of -4 dBm is found at 1484.86 nm and a minimum power of -8.2 dBm at 1607.8 nm resulting in a variation of 4.2 dBm across bandwidth. Such variation can be understood by noting that due to ISRS, $\eta_n(f_i)$ is higher for high wavelengths, even though these wavelengths suffer a greater dispersion. In contrast, P_{ASE_i} is higher for low wavelengths, as these wavelengths experience more loss due to the attenuation profile combined with the ISRS. Thus, especially because of the ISRS effect, more launch power are expected for low wavelengths, as these wavelengths experience more ASE noise and less nonlinear effects.

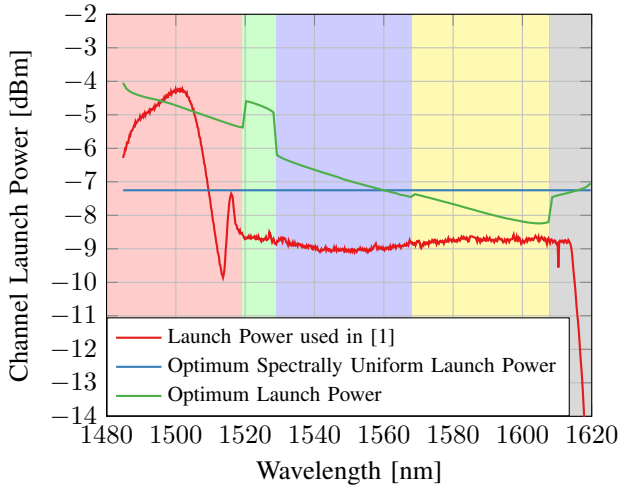

Fig. 2. Launch power per channel obtained from the optimisation described in Section III, using the model proposed in Section II. The launch power used in [1] is also shown for comparison.

Foremost, as described in details in [1], different amplification technologies, such as Thulium-doped fibre, discrete Raman and Erbium-doped fibre amplifiers, are utilized for different wavelengths ranges within the total transmission bandwidth. Each amplifier determines its operational wavelengths range and demonstrates different $\mathrm{NF_{ASE}}$ value, as shown in Table I. Therefore, we observe humps in the optimal power profile at different sub-bands highlighted by the different background colours, while maintaining the main trend of a downward slope. Indeed, to neutralise the undesired impact of higher ASE noise from the in-line amplifiers, higher launch power is required.

IV. System Performance

This section investigates the impact of launch power optimisation and the transceiver noise in the transmission system performance reported in [1]. For each launch power profile shown in Figure 2, the received SNR is illustrated in Figure 3.

The dashed lines show the SNR obtained by considering an ideal transceiver ($\mathrm{SNR_{TRX}} = \infty$). For the optimum launch power per channel optimisation case (green dashed line), the SNR varies between 31.59 dB and 35.37 dB. For the spectrally uniform launch power profile (blue dashed line), the SNR varies between 30.28 dB and 35.32 dB. For both cases, the minimum and maximum value of SNR occurred at 1607.8 nm and 1529.2 nm, respectively. Similar to Section III, the humps observed in the SNR profile at different sub-bands highlighted by the different background colours, relies on the different in-line amplifiers $\mathrm{NF_{ASE}}$ used to compensate for fibre loss; higher the NF, lower the SNR. Furthermore, the main trend of an upward slope is observed as the lower wavelength channels experience the lowest SNRs due to ISRS.

For the launch power used in the experiment (red dashed line), the SNR varies between 23.18 dB at 1619.67 nm and 34.86 dB at 1607.8 nm. This represents 11.68 dB variation in the SNR across the entire transmission bandwidth compared to only 3.78 dB variation for the optimum launch power profile case. Note that, for channels in the range of 1487-1508 nm, the SNR values are higher for the experiment case. This is due to the combination of two factors when compared with the optimum launch power per channel optimisation case. Firstly, because of their locally increased launch power. Secondly, because these channels transfer less power for the higher wavelengths channels. The latter occurs because of the reduced launch power used for channels above 1520 nm. This decreases the performance of these channels in exchange for an increase in performance for the channels between 1487-1508 nm. As result, a lower mean SNR and, therefore, a lower total throughput is obtained for the launch power used in the experiment compared with the other launch power profiles.

The continuous lines consider the inclusion of the noise introduced by the experiment back-to-back implementation penalty, as per Table I, for the different launch power profiles shown in Figure 2. Note that, when the transceiver noise is taken into account the mean SNR drops from 33.16 dB, when just the linear and non-linear noise generated by the in-line amplifiers and the optical fibre is taken into account (red dashed line), to 19.56 dB (red continuous line). Moreover, for the continuous lines, the difference in SNR among all three launch power cases is negligible.

It is clear that the transmission system performance under investigation is mainly limited by the transceiver noise. This can be explained by noting that $\kappa = 1/\mathrm{SNR_{TRX}}$ in equation (1) prevails under the remaining terms. This is generally the case for short-distance transmissions systems, where the nonlinear effects and the ASE noise are not so problematic compared with the noise introduced by the transceiver. The experimentally measured received SNR from [1] are depicted as grey marks for comparison, showing good agreement between the analytical model and the experimental results.

V. Conclusions

Future ultra-wideband WDM transmission systems will require the development of open and effective network planning tools. To that end, fast, accurate and reconfigurable computer models will be necessary. These models will allow an online assessment of the data rates, modulation formats, number of channels and launch power profile, given the fibre and the in-line amplifier characteristics.

In this paper, we demonstrate such assessment for the point-to-point transmission system, using the so-called ISRS GN model. Different launch power profiles has been investigated, and we concluded that for this particular 40 km transmission system, the transceiver noise is the predominant noise source, and as consequence different launch power optimisation (optimum spectrally uniform or optimum launch power per channel) had negligible impact on the per channel and overall system performance.

For future work, we will investigate the impact of launch power optimisation together with transceiver noise in an opti-

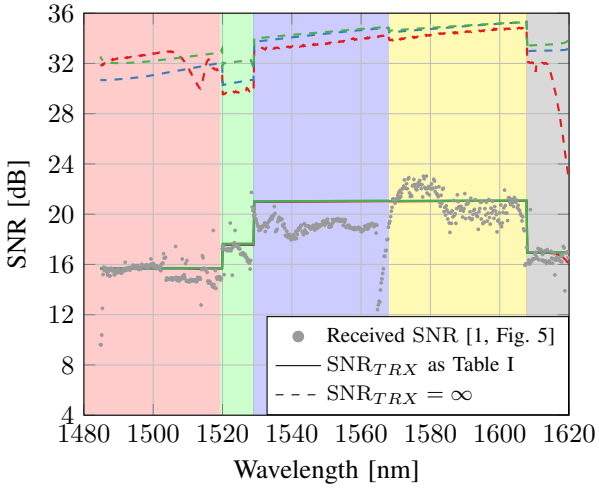

Fig. 3. SNR profile per channel for optimum launch power (green), optimum spectrally uniform launch power (blue) and launch power used in [1] (red). Two scenarios are considered: transceiver noise as Table I (continuous line) and the case of an ideal transceiver (dashed line). The experimental measurements in [1] (grey marks) are shown for comparison.

cal network scenario. Its impact on the quality-of-transmission (QoT) and link throughput will be analysed and strategies to maximise the efficiency of the existing network topologies will be proposed.

VI. Data Availability Statement

The data that supports the figures within this paper are available from the UCL Research Data Repository (DOI: 10.5522/04/14686794), which is hosted by FigShare.

References

[1] L. Galdino, A. Edwards, W. Yi, E. Sillekens, Y. Wakayama, T. Gerard, W. S. Pelouch, S. Barnes, T. Tsuritani, R. I. Killey *et al.*, "Optical fibre capacity optimisation via continuous bandwidth amplification and geometric shaping," *IEEE Photonics Technology Letters*, vol. 32, no. 17, pp. 1021–1024, 2020.

[2] F. Hamaoka, M. Nakamura, S. Okamoto, K. Minoguchi, T. Sasai, A. Matsushita, E. Yamazaki, and Y. Kisaka, "Ultra-wideband wdm transmission in s-, c-, and l-bands using signal power optimization scheme," *Journal of Lightwave Technology*, vol. 37, no. 8, pp. 1764–1771, 2019.

[3] J. Renaudier, A. C. Meseguer, A. Ghazisaeidi, P. Tran, R. R. Muller, R. Brenot, A. Verdier, F. Blache, K. Mekhazni, B. Duval, H. Debregeas, M. Achouche, A. Boutin, F. Morin, L. Letteron, N. Fontaine, Y. Frignac, and G. Charlet, "First 100-nm continuous-band wdm transmission system with 115tb/s transport over 100km using novel ultra-wideband semiconductor optical amplifiers," in *2017 European Conference on Optical Communication (ECOC)*, 2017, pp. 1–3.

[4] J. Renaudier, A. Arnould, D. L. Gac, A. Ghazisaeidi, P. Brindel, M. Makhsiyan, A. Verdier, K. Mekhazni, F. Blache, H. Debregeas, A. Boutin, N. Fontaine, D. Neilson, R. Ryf, H. Chen, M. Achouche, and G. Charlet, "107 tb/s transmission of 103-nm bandwidth over 3×100 km ssmf using ultra-wideband hybrid raman/soa repeaters," in *Optical Fiber Communication Conference (OFC) 2019*. Optical Society of America, 2019, p. Tu3F.2. [Online]. Available: http://www.osapublishing.org/abstract.cfm?URI=OFC-2019-Tu3F.2

[5] A. Sano, T. Kobayashi, S. Yamanaka, A. Matsuura, H. Kawakami, Y. Miyamoto, K. Ishihara, and H. Masuda, "102.3-tb/s (224 × 548-gb/s) c- and extended l-band all-raman transmission over 240 km using pdm-64qam single carrier fdm with digital pilot tone," in *National Fiber Optic Engineers Conference*. Optical Society of America, 2012, p. PDP5C.3. [Online]. Available: http://www.osapublishing.org/abstract.cfm?URI=NFOEC-2012-PDP5C.3

[6] L. Galdino, D. Semrau, M. Ionescu, A. Edwards, W. Pelouch, S. Desbruslais, J. James, E. Sillekens, D. Lavery, S. Barnes, R. I. Killey, and P. Bayvel, "Study on the impact of nonlinearity and noise on the performance of high-capacity broadband hybrid raman-edfa amplified system," *Journal of Lightwave Technology*, vol. 37, no. 21, pp. 5507–5515, 2019.

[7] M. Ionescu, D. Lavery, A. Edwards, E. Sillekens, D. Semrau, L. Galdino, R. I. Killey, W. Pelouch, S. Barnes, and P. Bayvel, "74.38 tb/s transmission over 6300 km single mode fibre enabled by c+l amplification and geometrically shaped pdm-64qam," *Journal of Lightwave Technology*, vol. 38, no. 2, pp. 531–537, 2020.

[8] J. . Cai, H. G. Batshon, M. V. Mazurczyk, C. R. Davidson, O. V. Sinkin, D. Wang, M. Paskov, W. W. Patterson, M. A. Bolshtyansky, and D. G. Foursa, "94.9 tb/s single mode capacity demonstration over 1,900 km with c+l edfas and coded modulation," in *2018 European Conference on Optical Communication (ECOC)*, 2018, pp. 1–3.

[9] J. . Cai, H. G. Batshon, M. V. Mazurczyk, O. V. Sinkin, D. Wang, M. Paskov, W. Patterson, C. R. Davidson, P. Corbett, G. Wolter, T. Hammon, M. Bolshtyansky, D. Foursa, and A. Pilipetskii, "70.4 tb/s capacity over 7,600 km in c+l band using coded modulation with hybrid constellation shaping and nonlinearity compensation," in *2017 Optical Fiber Communications Conference and Exhibition (OFC)*, 2017, pp. 1–3.

[10] J. Cai, Y. Sun, H. Zhang, H. G. Batshon, M. V. Mazurczyk, O. V. Sinkin, D. G. Foursa, and A. Pilipetskii, "49.3 tb/s transmission over 9100 km using c+l edfa and 54 tb/s transmission over 9150 km using hybrid-raman edfa," *Journal of Lightwave Technology*, vol. 33, no. 13, pp. 2724–2734, 2015.

[11] J. Cai, H. G. Batshon, M. V. Mazurczyk, O. V. Sinkin, D. Wang, M. Paskov, C. R. Davidson, W. W. Patterson, A. Turukhin, M. A. Bolshtyansky, and D. G. Foursa, "51.5 tb/s capacity over 17,107 km in c+l bandwidth using single-mode fibers and nonlinearity compensation," *Journal of Lightwave Technology*, vol. 36, no. 11, pp. 2135–2141, 2018.

[12] D. Semrau, R. I. Killey, and P. Bayvel, "A closed-form approximation of the gaussian noise model in the presence of inter-channel stimulated raman scattering," *Journal of Lightwave Technology*, vol. 37, no. 9, pp. 1924–1936, 2019.

[13] J. Kennedy and R. Eberhart, "Particle swarm optimization," in *Proceedings of ICNN'95 - International Conference on Neural Networks*, vol. 4, 1995, pp. 1942–1948 vol.4.

[14] D. Semrau, E. Sillekens, P. Bayvel, and R. I. Killey, "Modeling and mitigation of fiber nonlinearity in wideband optical signal transmission," *IEEE/OSA Journal of Optical Communications and Networking*, vol. 12, no. 6, pp. C68–C76, 2020.